

Dynamic boundary conditions and boundary layer approach to the wind-driven, linear circulation problem

L. CASTELLANA, F. CRISCIANI and R. PURINI

Istituto Talassografico del CNR - Trieste, Italy

(ricevuto il 12 Maggio 2000; revisionato il 22 Novembre 2000; approvato il 23 Gennaio 2001)

Summary. — Boundary layer techniques are applied to a class of wind-driven, linear circulation models in which a wide set of dynamic boundary conditions are allowed. The results show that i) the eastern solution always exists and its $O(1)$ component coincides with that of Sverdrup; ii) only a well-defined subset of boundary conditions are consistent with solutions representing, at least qualitatively, a typical subtropical gyre and, finally, iii) it is possible to employ infinite choices of boundary conditions which correspond to the same boundary layer solution.

PACS 92.10.Fj – Dynamics of the upper ocean.

PACS 47.10 – Fluid dynamics: general theory.

1. – Introduction

Linear, wind-driven circulation models for a homogeneous ocean started with the pioneering work of Henry Stommel [1] who, first, gave the basic explanation of the westward intensification of a surface-forced ocean. The dynamical balance of the western area was obtained by resorting to the most simple parametrization of turbulence, mathematically described by a Laplacian operator acting on the streamfunction. This operator does not raise the order of the differential vorticity equation, so no additive boundary conditions were necessary besides these of no mass flux to be applied along the impermeable coastline. The key ingredients singled out by Stommel, that is the beta effect together with turbulent dissipation, was later investigated by Walter Munk [2] by resorting to another kind of parametrization, the so-called lateral diffusion of relative vorticity and defined mathematically by a Laplacian operator acting on the relative vorticity field. In spite of the great number of circulation models taken into account from 1950 up to now using this frictional mechanism and the enormous progress in numerical techniques, the central difficulty of formulating a fully deductive circulation model has been not solved because of the inherent indeterminacy of the dynamic boundary conditions which must be invoked to close the problem. It is well known that nonlinearity is a further complication which does not help us in facing with such indeterminacy, so, in the present paper, we wish to explore the situation in the linear context, where the powerful boundary layer technique

can be applied. Indeed, also this technique is far from being original. In fact it can be used in a wide spectrum of linear models, but, in general, each model is necessarily characterized by definite dynamic boundary conditions in order to be univocally posed. The present approach is somehow different, in the sense that we introduce a 3-parameter class of dynamic boundary conditions into the problem and explore the boundary layer solutions depending on these parameters.

2. – Dynamical framework

In what follows we consider the wind-driven circulation problem in the steady and linearized form, *i.e.* governed by the well-known nondimensional vorticity equation

$$(2.1) \quad \frac{\partial \psi}{\partial x} = \text{curl } \vec{\tau} + \left(\frac{\delta}{L} \right)^3 \nabla^4 \psi,$$

for a flow field included into the square fluid domain $D = [0 \leq x \leq 1] \times [0 \leq y \leq 1]$. Equation (2.1) is obtained by means of a standard scaling and nondimensionalization procedure applied to the Navier-Stokes primitive equations in which the horizontal length scale L and the typical horizontal velocity U are taken in accordance with the basin-scale phenomenology. In (2.1) δ is related to the dimensional Austausch dimensional coefficient A_H by the equation $A_H = \beta \delta^3$, where β is the planetary vorticity gradient.

The no mass flux boundary condition (hereafter b.c.) has the form

$$(2.2) \quad \psi = 0 \quad \forall (x, y) \in \partial D.$$

The forcing field of the model has the typical profile, sinusoidal with respect to latitude, *i.e.*

$$\text{curl } \vec{\tau} = -\pi \sin(\pi y).$$

The Sverdrup solution ψ_I is defined by the problem

$$(2.3) \quad \begin{cases} \frac{\partial \psi_I}{\partial x} = \text{curl } \vec{\tau}, \\ \psi_I(x_b, y) = 0, \end{cases}$$

where we have still to decide whether $x_b = 0$ or $x_b = 1$. Obviously, we already know that the correct solution is $x_b = 1$, for instance from the theory of Rossby waves propagation [3, 4]; however we wish to recover this feature also in the context of the present approach and the answer will follow from the analysis of the solution close to the eastern boundary.

In any case, (2.3) yields

$$(2.4) \quad \psi_I(x, y) = \pi(x_b - x) \sin(\pi y).$$

The key point of the following discussion arises from the presence of the term describing the lateral diffusion of relative vorticity, *i.e.* $(\delta/L)^3 \nabla^4 \psi$ which demands *additional* (so-called dynamical) b.c.'s, to be specified. Since we are interested in the investigation of

the zonal structure of the flow field by means of boundary layer techniques, in what follows we impose free-slip b.c.'s in $y = 0$ and $y = 1$ in order to make the problem for the meridional flow as simple as possible. Note that the partial solution (2.4) alone does satisfy the no mass flux and free-slip b.c.'s along the zonal boundaries.

For what concerns the dynamic b.c.'s to be applied to the meridional boundaries, we take into account a linear combination of the well-known no-slip, free-slip and superslip b.c.'s, of the form

$$(2.5) \quad C_1 \frac{\partial \psi}{\partial x} + C_2 \nabla^2 \psi + C_3 \frac{\partial}{\partial x} \nabla^2 \psi = 0 \quad \text{in } x = 0 \text{ and } x = 1.$$

Each term (C_1, C_2, C_3) corresponds to a definite dynamic b.c. but, unlike the common method in which a definite choice is fixed *a priori* (for instance $(1, 0, 0)$ for the no-slip b.c.), here we wish to deal with a class of b.c. as a whole and to take conclusions from this approach. On this subject, we recall also Stewart's theorem [5], reported also in Pedlosky [6] that takes the following dimensional form:

$$(2.6) \quad \frac{f_0}{D} \int_{y_1}^{y_2} \int_0^{x_E} w \, dx \, dy = A_H \int_{y_1}^{y_2} \frac{\partial}{\partial x} \zeta(0, y) \, dy.$$

Theorem (2.6) states that the vorticity put in the basin by the wind inside the latitudinal strip $[y_1, y_2]$ is fluxed out by dissipation at the same latitudinal strip. In our investigation, we allow the flux to be expressed as a linear combination of the kind

$$\frac{\partial}{\partial x} \zeta(0, y) = \frac{\partial}{\partial x} \left[\alpha_1 \frac{\psi(0, y)}{\delta^2} + \alpha_2 \frac{v(0, y)}{\delta} \right],$$

where the coefficients α_i ($i = 1, 2$) are related in an obvious way to those appearing in (2.5).

3. – The boundary layer approach on the eastern boundary

First of all, we introduce the boundary layer stretching coordinate λ for the eastern boundary by setting

$$(3.1) \quad \delta \lambda = L(x - 1).$$

As a consequence of (3.1) we have

$$(3.2) \quad \frac{\partial}{\partial x} = \frac{L}{\delta} \frac{\partial}{\partial \lambda}.$$

In the eastern area the solution is written in terms of the superposition of the interior solution (2.4) plus an eastern boundary layer solution $\phi_E(\lambda, y)$ as

$$(3.3) \quad \psi(x, y) = \psi_I(x, y) + \phi_E(\lambda, y).$$

The correction $\phi_E(\lambda, y)$ must satisfy the matching condition of ψ with the interior ψ_I , *i.e.*

$$(3.4) \quad \lim_{\lambda \rightarrow -\infty} \phi_E(\lambda, y) = 0$$

and the no mass flux boundary condition

$$(3.5) \quad \psi_I(1, y) + \phi_W(0, y) = 0.$$

At this point, we have all the rules to infer the vorticity equation of $\phi_E(\lambda, y)$ starting from the substitution of (3.3) into (2.1), by using also (2.4), (3.2). The result is

$$(3.6) \quad \frac{L}{\delta} \frac{\partial \phi_E}{\partial \lambda} = \left(\frac{\delta}{L}\right)^3 \left\{ \nabla^4 \psi_I + \left(\left(\frac{L}{\delta}\right)^2 \frac{\partial^2}{\partial \lambda^2} + \frac{\partial^2}{\partial y^2} \right) \left[\left(\frac{L}{\delta}\right)^2 \frac{\partial^2 \phi_E}{\partial \lambda^2} + \frac{\partial^2 \phi_E}{\partial y^2} \right] \right\}$$

and the balance between the dominant terms, *i.e.* $O(L/\delta)$ in (3.6) takes the form

$$(3.7) \quad \frac{\partial \phi_E}{\partial \lambda} = \frac{\partial^4 \phi_E}{\partial \lambda^4}.$$

From (3.4) and (3.7) we obtain $\phi_E(\lambda, y) = A(y) \exp[\lambda]$ and hence

$$(3.8) \quad \psi = \psi_I(x, y) + A(y) \exp[\lambda].$$

Now, we transform (2.5) in function of the variables x, λ, y as follows:

$$(3.9) \quad C_1 \frac{\partial \psi_I}{\partial x} + C_1 \frac{L}{\delta} \frac{\partial \phi_E}{\partial \lambda} + C_2 \nabla^2 \psi_I + C_2 \left[\left(\frac{L}{\delta}\right)^2 \frac{\partial^2}{\partial \lambda^2} + \frac{\partial^2}{\partial y^2} \right] \phi_E + \\ + C_3 \frac{\partial}{\partial x} \nabla^2 \psi_I + C_3 \frac{L}{\delta} \frac{\partial}{\partial \lambda} \left[\left(\frac{L}{\delta}\right)^2 \frac{\partial^2}{\partial \lambda^2} + \frac{\partial^2}{\partial y^2} \right] \phi_E = 0.$$

To avoid that the different order of magnitude of the powers of L/δ select only a few terms in (3.9) that would appear to be dominant if we do not state definite hypotheses on C_i , we fix the order of magnitude of C_i such that $C_i = (\delta/L)^i K_i$, $i = 1, 2, 3$, where

$$(3.10) \quad K_i = O(1) \quad \text{and} \quad \sum_1^3 K_i \neq 0.$$

Therefore (3.9) takes the form

$$(3.11) \quad K_1 \frac{\delta}{L} \frac{\partial \psi_I}{\partial x} + K_1 \frac{\partial \phi_E}{\partial \lambda} + K_2 \left(\frac{\delta}{L}\right)^2 \nabla^2 \psi_I + K_2 \left[\frac{\partial^2}{\partial \lambda^2} + \left(\frac{\delta}{L}\right)^2 \frac{\partial^2}{\partial y^2} \right] \phi_E + \\ + K_3 \left(\frac{\delta}{L}\right)^3 \frac{\partial}{\partial x} \nabla^2 \psi_I + K_3 \left[\frac{\partial^3}{\partial \lambda^3} + \left(\frac{\delta}{L}\right)^3 \frac{\partial^3}{\partial \lambda \partial y^2} \right] \phi_E = 0.$$

Substitution of (3.8), evaluated in $x = 1$, $\lambda = 0$, into (3.11) and disregarding in (3.11) the terms $O(\delta^2/L^2)$, yields

$$(3.12) \quad \frac{\delta}{L} K_1 \operatorname{curl} \bar{\tau}(y) + A(y) \sum_1^3 K_i = 0.$$

From (3.8), (3.12) we have the total solution

$$(3.13) \quad \psi = \psi_1(x, y) - \frac{\delta}{L} \frac{K_1}{\sum_1^3 K_i} \operatorname{curl} \bar{\tau}(y) \exp[\lambda].$$

To the zeroth order in δ/L the no mass flux b.c. (3.5) applied to (3.13) simply gives $\psi_1(1, y) = 0$. This fact, well known in the literature, states that “The Sverdrup solution must ... itself satisfy the condition of no normal flow on the oceanic eastern boundary” [4]. Then, with reference to (2.5), we identify x_b with the eastern longitude of the basin in accordance with the anticipation reported in sect. 2.

We can check that solution (3.13) does satisfy our generalized b.c. (3.11) up to the first order in δ/L : in fact, putting (3.13) into (3.11), within the above approximation we obtain

$$\frac{\delta}{L} K_1 \operatorname{curl} \bar{\tau}(y) - \frac{\delta}{L} \frac{K_1^2}{\sum_1^3 K_i} \operatorname{curl} \bar{\tau}(y) - \frac{\delta}{L} \frac{K_1 K_2}{\sum_1^3 K_i} \operatorname{curl} \bar{\tau}(y) - \frac{\delta}{L} \frac{K_1 K_3}{\sum_1^3 K_i} \operatorname{curl} \bar{\tau}(y) = 0$$

and thus the identity

$$K_1 - \frac{K_1^2}{\sum_1^3 K_i} - \frac{K_1 K_2}{\sum_1^3 K_i} - \frac{K_1 K_3}{\sum_1^3 K_i} = 0$$

follows. In particular, if we consider the special case of no-slip b.c. which corresponds to $K_1 = 1$, $K_2 = K_3 = 0$, eq. (3.13) gives $\psi = \psi_1(x, y) - (\delta/L) \operatorname{curl} \bar{\tau}(1, y) \exp[\lambda]$ which coincides with the solution found in Pedlosky [4], eq. (5.4.22).

The main conclusion of the present section is that *all the dynamic b.c.'s which can be summarized into (2.5) are consistent with the existence of boundary layer solutions along the eastern boundary of the ocean.*

4. – The boundary layer approach on the western boundary

4.1. *Conditions for the existence of boundary layer solutions.* – In analogy with the method followed for the eastern boundary, we define the transform

$$(4.1) \quad \delta\lambda = Lx,$$

which implies again (3.2) while the total solution is now written as

$$(4.2) \quad \psi(x, y) = \psi_1(x, y) + \phi_W(\lambda, y),$$

where $\phi_W(\lambda, y)$ is the western boundary layer correction.

The equation for $\phi_W(\lambda, y)$ is

$$(4.3) \quad \frac{L}{\delta} \frac{\partial \phi_W}{\partial \lambda} = \left(\frac{\delta}{L}\right)^3 \left\{ \nabla^4 \psi_I + \left(\left(\frac{L}{\delta}\right)^2 \frac{\partial^2}{\partial \lambda^2} + \frac{\partial^2}{\partial y^2}\right) \left[\left(\frac{L}{\delta}\right)^2 \frac{\partial^2 \phi_W}{\partial \lambda^2} + \frac{\partial^2 \phi_W}{\partial y^2}\right] \right\}.$$

The problem for $\phi_W(\lambda, y)$ is determined by (4.3), the relation

$$(4.4) \quad \lim_{\lambda \rightarrow +\infty} \phi_W(\lambda, y) = 0,$$

and the no mass flux b.c. in $x = 0, \lambda = 0$, *i.e.*

$$(4.5) \quad \psi_I(0, y) + \phi_W(0, y) = 0.$$

To the leading-order term, (4.3) simplifies into

$$(4.6) \quad \frac{\partial \phi_W}{\partial \lambda} = \frac{\partial^4 \phi_W}{\partial \lambda^4}.$$

The integral of (4.6) which verifies (4.4) and (4.5) has the form

$$(4.7) \quad \phi_W = B(y) \sin\left(\frac{\sqrt{3}}{2}\lambda\right) \exp\left[-\frac{\lambda}{2}\right] - \psi_I(0, y) \cos\left(\frac{\sqrt{3}}{2}\lambda\right) \exp\left[-\frac{\lambda}{2}\right].$$

The generalized form of the dynamic b.c. is, also in this case, (3.11) with $\phi_W(\lambda, y)$ in place of $\phi_E(\lambda, y)$. At the zeroth order in δ/L , substitution of (4.2) with ϕ_W given by (4.7) yields

$$(4.8) \quad \sqrt{3}B(y)(K_1 - K_2) + \psi_I(0, y)(K_1 + K_2 - 2K_3) = 0.$$

Equation (4.8) gives the last unknown of the problem, *i.e.* $B(y)$ as a function of $\psi_I(0, y)$ and K_i . Note that the very existence of a nonvanishing wind field demands that $K_1 - K_2 \neq 0$. If

$$(4.9) \quad K_1 - K_2 = 0 \quad \text{and} \quad K_1 + K_2 - 2K_3 = 0,$$

then (4.8) would be undetermined (this happens for $K_1 = K_2 = K_3$). In particular the superslip condition, corresponding to $K_1 = K_2 = 0$ and $K_3 = 1$ does not allow a boundary layer treatment [6].

4.2. Range of K_i corresponding to physical solutions. – In this section, we consider the solution

$$(4.10) \quad \psi(x, y) = \psi_I(x, y) - \psi_I(0, y) \times \\ \times \exp\left[-\frac{L}{2\delta}x\right] \left[\frac{K_1 + K_2 - 2K_2}{\sqrt{3}(K_1 - K_2)} \sin\left(\frac{\sqrt{3}}{2}\frac{L}{\delta}x\right) + \cos\left(\frac{\sqrt{3}}{2}\frac{L}{\delta}x\right)\right],$$

which refers to the western and interior area of our basin and it is derived from (4.2) and (4.7) with $B(y)$ given by (4.8). The western boundary layer coordinate λ has been

TABLE I. – Range of the parameter H corresponding to gyre-like solutions for different strengths of the lateral dissipation.

δ/L	Range of H
10^{-1}	$[-8.0; 1.4]$
$5 \cdot 10^{-2}$	$[-4.0; 1.5]$
$2.5 \cdot 10^{-2}$	$[-1.4; 1.5]$

expressed in terms of the longitude x by using (4.1). Actually, solution (4.10) is, to a good extent, valid for the whole fluid domain since the eastern boundary layer correction ϕ_E contributes only with a term of the order of δ/L .

Once the forcing is fixed, ψ_I is completely known and every option within the set of dynamic b.c.'s (2.6) singles out a special value of the quantity

$$(4.11) \quad H \equiv \frac{K_1 + K_2 - 2K_3}{\sqrt{3}(K_1 - K_2)}$$

(recall that $C_i = (\delta/L)^i K_i$, $i = 1, 2, 3$). However, not all the values which can be attributed to H lead to solutions (4.10) corresponding, at least qualitatively, to a typical subtropical gyre. In accordance with a well-known phenomenology (see, for instance, [7]) we expect a westward intensified flow field with a marked northward current close to the western boundary and a weak southward current which extends from the interior to the eastern side of the basin. On such criterion, we discarded values of H which yielded negative ψ for some $x \in [0, 1]$ and negative $\partial\psi/\partial x$ far from the western boundary. To apply these criteria and to determine the range of H , we have done a set of numerical simulations of the solution and the associated meridional current, both evaluated at the middle basin latitude $y = 0.5$, with $\delta/L = 10^{-1}$, $5 \cdot 10^{-2}$, $2.5 \cdot 10^{-2}$. An accepted value of δ/L is $5 \cdot 10^{-2}$ but, in any case, we have tested the sensitivity of the solution in a suitable range including it. The results of the simulations leading to acceptable solutions are summarized in table I. The extremes of each range are truncated at the first significative digit.

Figures from 1a) to 3b) show the meridional part of the solutions and the associated meridional currents corresponding to the values of δ/L and to the extremes of H , listed in table I. These solutions allow us to evaluate two-dimensional quantities which can be compared with observational data (for instance of the Gulf Stream), *i.e.* the maximum northward velocity $v_* = Uv$ of the fluid in the western area and the northward transport $M_* = HLU\psi_{\text{Max}}$ in the western boundary. For $U = 2 \cdot 10^{-2}$ m/s [4], and using the data of fig. 1b), 2b) and 3b) we have, respectively, $0.28 \text{ m/s} \leq v_* \leq 1.68 \text{ m/s}$, $0.64 \text{ m/s} \leq v_* \leq 2 \text{ m/s}$, $1.32 \text{ m/s} \leq v_* \leq 2.2 \text{ m/s}$. On the whole, these velocities are consistent with observations ($v_* \approx 1 \text{ m/s}$). To estimate $M_* = HLU\psi_{\text{Max}}$ we assume the depth of the moving fluid to be of the order of 10^3 m and $L = 10^6$ m [4], so $HLU = 10 \text{ Sv}$. Using the data of figs. 1a), 2a) and 3a) we have, respectively, $26 \text{ Sv} \leq M_* \leq 62 \text{ Sv}$, $31 \text{ Sv} \leq M_* \leq 44 \text{ Sv}$, $34 \text{ Sv} \leq M_* \leq 38 \text{ Sv}$. We recall that the observed transport of the Gulf Stream varies with latitude from about 30 to 100 Sv [8], so our results are not too far from observational data.

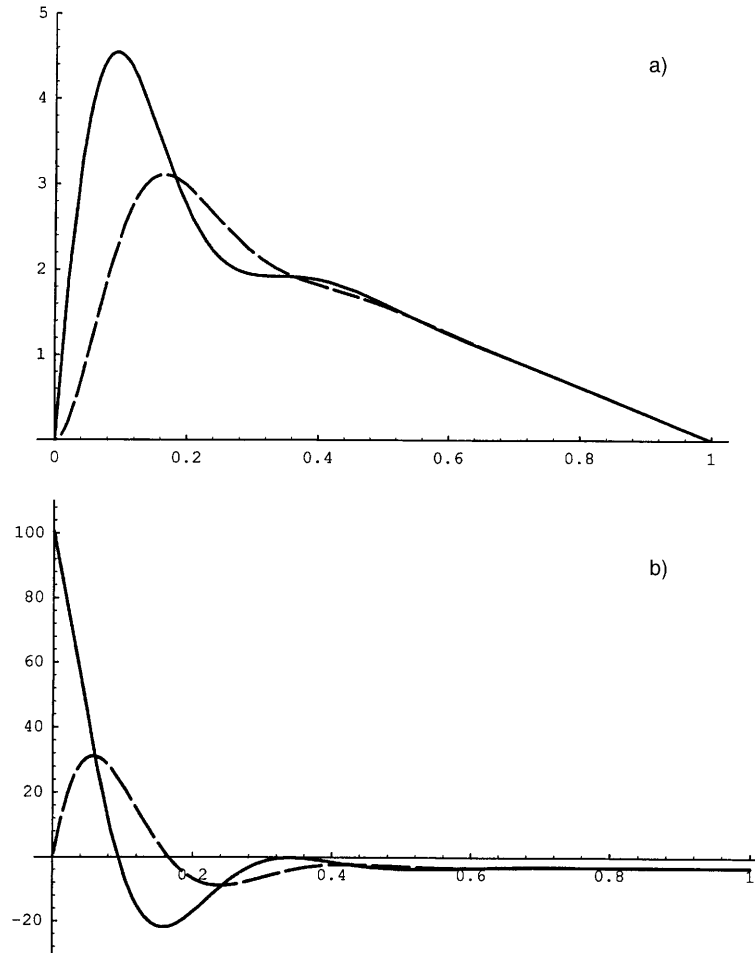


Fig. 1. – a) Plots of $\psi(x, 1/2)$ evaluated for $\delta/L = 10^{-1}$, $H = -4.6$ (continuous line) and $H = 0.8$ (dashed line). All the plots corresponding to $-4.6 < H < 0.8$ are included between the continuous and the dashed lines. The two maxima of $\psi(x, 1/2)$ are 6.2 and 2.6, respectively. b) Plots of $[\partial\psi/\partial x]_{y=1/2}$ evaluated for $\delta/L = 10^{-1}$, $H = -4.6$ (continuous line) and $H = 0.8$ (dashed line). All the plots corresponding to $-4.6 < H < 0.8$ are included between the continuous and the dashed lines. The two maxima of $[\partial\psi/\partial x]_{y=1/2}$ are 84 and 14, respectively.

5. – Admissible dynamic boundary conditions for a given solution

Equation (4.11) relates the amplitude H of the term $\exp[-(L/2\delta)x] \sin((\sqrt{3}/2)(L/\delta)x)$ appearing into solution (4.10) to the coefficients K_i which single out each specific b.c. through (3.10). It is already intuitive from (4.11) itself that different terms (K_1, K_2, K_3) correspond to the same H , and therefore to the same solution (4.10). This situation can be clarified if we rewrite (4.11) under the form

$$(5.1) \quad (\sqrt{3}H - 1)K_1 - (\sqrt{3}H + 1)K_2 + 2K_3 = 0$$

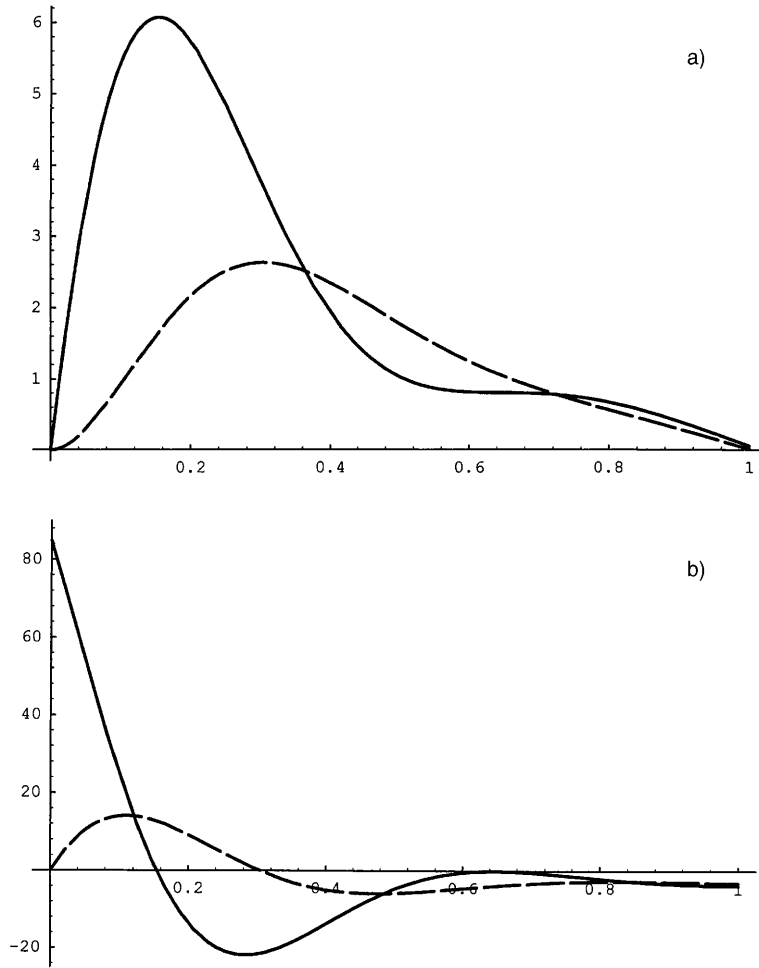


Fig. 2. - a) Plots of $\psi(x, 1/2)$ evaluated for $\delta/L = 5 \cdot 10^{-2}$, $H = -2.3$ (continuous line) and $H = 0.9$ (dashed line). All the plots corresponding to $-2.3 < H < 0.9$ are included between the continuous and the dashed lines. The two maxima of $\psi(x, 1/2)$ are 4.4 and 3.1, respectively. b) Plots of $[\partial\psi/\partial x]_{y=1/2}$ evaluated for $\delta/L = 5 \cdot 10^{-2}$, $H = -2.3$ (continuous line) and $H = 0.9$ (dashed line). All the plots corresponding to $-2.3 < H < 0.9$ are included between the continuous and the dashed lines. The two maxima of $[\partial\psi/\partial x]_{y=1/2}$ are 100 and 32, respectively.

and regard the lhs of (5.1) as the dot product $\vec{H} \cdot \vec{K}$, where we have introduced the vectors $\vec{H} = (\sqrt{3}H - 1, -\sqrt{3}H - 1, 2)$ and $\vec{K} = (K_1, K_2, K_3)$. Equation (5.1) states an orthogonality relation between \vec{H} and \vec{K} in which \vec{H} can be considered fixed while \vec{K} is determined by the requests that it belongs to a plane orthogonal to the vector \vec{H} and that $|\vec{K}| = O(1)$ (recall (3.10)). For instance \vec{K} can belong to the plane of equation

$$(5.2) \quad (1 - \sqrt{3}H)K_1 + (1 + \sqrt{3}H)K_2 - 2K_3 = 0.$$

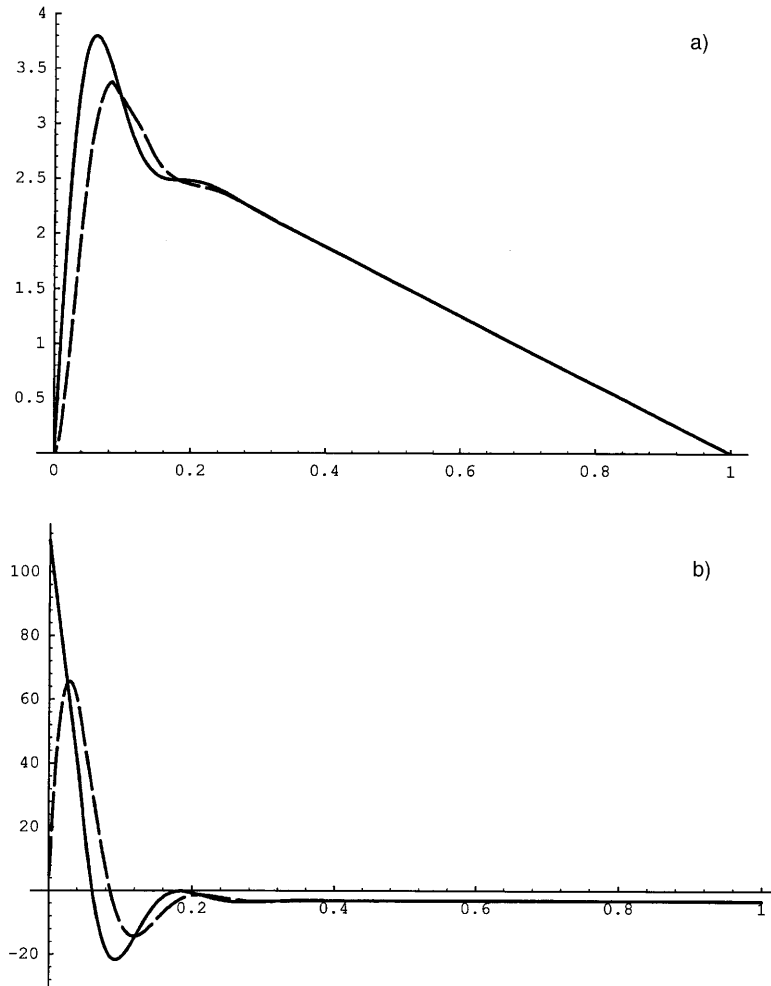


Fig. 3. – a) Plots of $\psi(x, 1/2)$ evaluated for $\delta/L = 2.5 \cdot 10^{-2}$, $H = -0.8$ (continuous line) and $H = 0.9$ (dashed line). All the plots corresponding to $-0.8 < H < 0.9$ are included between the continuous and the dashed lines. The two maxima of $\psi(x, 1/2)$ are 3.8 and 3.4, respectively. b) Plots of $[\partial\psi/\partial x]_{y=1/2}$ evaluated for $\delta/L = 2.5 \cdot 10^{-2}$, $H = -0.8$ (continuous line) and $H = 0.9$ (dashed line). All the plots corresponding to $-0.8 < H < 0.9$ are included between the continuous and the dashed lines. The two maxima of $[\partial\psi/\partial x]_{y=1/2}$ are 110 and 66, respectively.

Therefore, for a given $|\vec{K}|$, say

$$(5.3) \quad |\vec{K}| = 1$$

we have from (5.2), (5.3) a one-parameter family of vectors, $\vec{K}(\theta)$ and hence ∞^1 dynamic b.c.'s that, together with (2.1) and (2.2), yields the same solution (4.10). The situation is depicted in fig. 4. If $|\vec{K}|$ varies into an interval (a, b) , where both $a = O(1)$ and $b = O(1)$, we have a two-parameter family of vectors, $\vec{K}(\theta, \rho)$ but the same conclusion as above

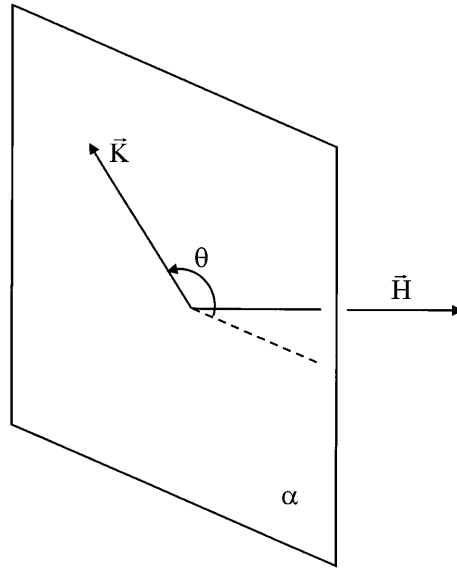


Fig. 4. – Sketch of a generic plane (α) normal to the vector \vec{H} to which the family of vectors $\vec{K}(\theta)$ belongs for a suitably varying “angle” θ .

would follow. In other words, even if an observational data set would be so accurate to trace back exactly solution (4.10), we would be unable to infer *in a univocal* way from (4.10) the dynamical b.c.’s leading to this solution.

6. – The role of bottom friction

If bottom friction is added to (2.1), and the same strength of dissipation is assumed both for lateral diffusion of relative vorticity and bottom friction, (2.1) modifies into

$$\frac{\partial \psi}{\partial x} = \text{curl } \vec{\tau} + \left(\frac{\delta}{L}\right)^3 \nabla^4 \psi - \frac{\delta}{L} \nabla^2 \psi$$

and the boundary layer equations (3.7), (4.6) takes the form

$$\frac{\partial \phi_A}{\partial \lambda} = \frac{\partial^4 \phi_A}{\partial \lambda^4} - \frac{\partial^2 \phi_A}{\partial \lambda^2}$$

for both the boundaries. This means that bottom dissipation introduces the further term $-(\partial^2 \phi_A / \partial \lambda^2)$. The presence of this special dissipative mechanism does not change the main features of the eastern solution, which is not very different from that reported at the end of sect. 3.

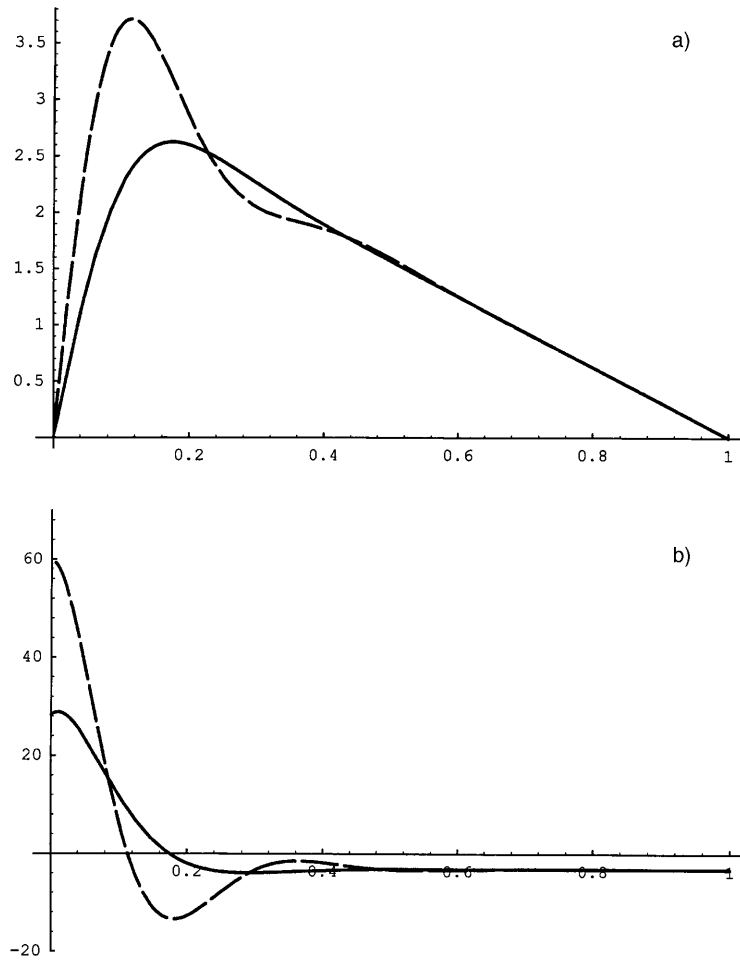


Fig. 5. - a) Plots of $\psi(x, 1/2)$ evaluated for $\delta/L = 5 \cdot 10^{-2}$, with bottom friction (continuous line) and without bottom friction (dashed line). All the plots correspond to $K_1 = K_3 = 1$, $K_2 = 0$ and we have (by using (6.5)) $H = (4a - 9a\omega^2 + a^3)/(\sqrt{3}\omega(4 + 3a^2 - 3\omega^2))$ in the first case and (by using (4.11)) $H = -(1/\sqrt{3})$ in the second. b) Plots of $[\partial\psi/\partial x]_{y=1/2}$ corresponding to the cases of panel a).

About the western boundary, instead of (4.8) we have the equation

$$(6.1) \quad \frac{\sqrt{3}}{2}\omega B(y) \left[K_1 - aK_2 + \left(\frac{3}{4}a^2 - \frac{3}{4}\omega^2 \right) K_3 \right] + \psi_I(0, y) \left[\frac{1}{2}aK_1 - \left(\frac{a^2}{4} - \frac{3}{4}\omega^2 \right) K_2 - \left(\frac{9}{8}a\omega^2 - \frac{1}{8}a^3 \right) K_3 \right] = 0,$$

where

$$a \equiv \left[\frac{1}{2} + \left(\frac{23}{108} \right)^{1/2} \right]^{1/3} + \left[\frac{1}{2} - \left(\frac{23}{108} \right)^{1/2} \right]^{1/3} \quad (\approx 1.3)$$

and

$$\omega \equiv \left[\frac{1}{2} + \left(\frac{23}{108} \right)^{1/2} \right]^{1/3} - \left[\frac{1}{2} - \left(\frac{23}{108} \right)^{1/2} \right]^{1/3} \quad (\approx 0.6).$$

The function $B(y)$ exists provided that

$$4K_1 - 4aK_2 + 3K_3(a^2 - \omega^2) \neq 0.$$

Moreover, (6.1) is left indetermined if

$$(6.2) \quad 4K_1 - 4aK_2 + 3K_3(a^2 - \omega^2) = 0$$

and

$$(6.3) \quad 4aK_1 - 2K_2(a^2 - 3\omega^2) - (9a\omega^2 - a^3)K_3 = 0.$$

From (6.2), (6.3) the condition of indeterminacy becomes

$$(6.4) \quad K_1 = aK_2 + \frac{3}{4}K_3(\omega^2 - a^2) \quad \text{and} \quad K_2 = aK_3.$$

Note that (6.4) reduces to (4.9) for $a = \omega = 1$, *i.e.* if bottom friction is ignored.

In the presence of bottom friction, the superslip b.c. is admissible since for $K_1 = K_2 = 0$ and $K_3 = 1$, (6.1) gives

$$B(y) = -\psi_1(0, y) \frac{a^3 - 9a\omega^2}{3\sqrt{3}\omega(a^2 - \omega^2)} \approx 0.5 \psi_1(0, y).$$

Another relevant difference is a general extension of the range of H corresponding to physically realistic solutions. We stress that, in the present situation, the dependence of H on K_i is

$$(6.5) \quad H = \frac{4aK_1 - 2K_2(a^2 - 3\omega^2) - (9a\omega^2 - a^3)K_3}{\sqrt{3}\omega \left[4K_1 - 4aK_2 + 3K_3(a^2 - \omega^2) \right]}.$$

The ranges are shown in table II. Note the marked decrease of the lower extreme with respect to the results of table I.

TABLE II. – Range of the parameter H corresponding to gyre-like solutions for different strengths of the lateral dissipation in the presence of bottom friction.

δ/L	Range of H
10^{-1}	$[-41.6; 1.1]$
$5 \cdot 10^{-2}$	$[-21.8; 1.2]$
$2.5 \cdot 10^{-2}$	$[-11.4; 1.2]$

We end this investigation with an example of two solutions, with and without bottom friction, having the same value $\delta/L = 5 \cdot 10^{-2}$ and $K_1 = K_3 = 1$, $K_2 = 0$. The profiles of $\psi(x, 1/2)$, evaluated within the boundary layer approximation, are reported in fig. 5a) (the continuous line corresponds to the presence of bottom friction while the dashed line is referred to the case without bottom friction). The damping due to bottom friction and the sharper peak of the solution in the other case is quite evident. This last is related to a marked meridional countercurrent, pointed out in fig. 5b) (where the same drawing convention as fig. 5a) is used) which does not appear if the northward transport is damped by bottom friction.

7. – Conclusions

The main results of the present investigation can be summarized as follows:

- Whatever the dynamic boundary conditions may be (in the considered class), the eastern solution always exists and its $O(1)$ component is that of Sverdrup.
- We have singled out the set of dynamic boundary conditions whose associated western circulation model *cannot* be solved by means of boundary layer techniques.
- If we require that our solution be comparable with the shape of a realistic subtropical gyre, the parameters of each element of the class must be properly confined into well-defined ranges.
- Given a boundary layer solution, there exist at least ∞^1 boundary conditions leading to such solution.

* * *

The authors are grateful to an anonymous referee for useful comments.

REFERENCES

- [1] STOMMEL H., *Trans. Am. Geophys. Union*, **29** (1948) 202.
- [2] MUNK W. H., *J. Meteor.*, **7** (1950) 79.
- [3] PEDLOSKY J., *J. Marine Res.*, **23** (1965) 207.
- [4] PEDLOSKY J., *Geophysical Fluid Dynamics* (Springer-Verlag) 1987, p. 710.
- [5] STEWART R. W., *The influence of friction on inertial models of oceanic circulation*, in *Studies in Oceanography: Papers Dedicated to Professor Hidaka in Commemoration of his 60th Birthday*, edited by K. YOSHIDA (Tokyo University, Geophys. Inst.) 1964, pp. 3-9.
- [6] PEDLOSKY J., *Ocean Circulation Theory* (Springer-Verlag) 1996, p. 453.
- [7] SCHMITZ W. I. and MCCARTNEY M. S., *Rev. Geophys.*, **31** (1993) 29.
- [8] HOLLAND W. R. and HIRSHMAN A. D., *J. Phys. Oceanogr.*, **2** (1972) 336.